

$$\rho_1 \frac{1}{2} (v_1^2 - v_0^2) = \rho_2 \frac{1}{2} (v_2^2 - v_0^2).$$

From the general law,

$$\frac{P_1}{P_2} = \frac{\rho_1 R T_1}{\rho_2 R T_2}.$$

For $P_1 = P_2$, $\rho_1 = \frac{\rho_2 T_2}{T_1}$. Substituting,

$$\rho_2 \frac{T_2}{T_1} (v_1^2 - v_0^2) = \rho_2 (v_2^2 - v_0^2). \quad \text{Hence,}$$

$$T_2 (v_1^2 - v_0^2) = T_1 (v_2^2 - v_0^2).$$

The relative velocity of one stratum, $(v_1^2 - v_0^2)$, multiplied by the temperature of the second, T_2 , equals the relative velocity of the second stratum, $(v_2^2 - v_0^2)$, multiplied by the temperature of the first, T_1 ; and this maintains the pressure as if the air had no motion, and the temperature gradients remained normal. The first type of vortex with the funnel-shaped tube depends upon the first principle more than upon the second, while the second type of vortex with the dumb-bell tube depends upon the second rather than upon the first. This will be illustrated by the Chamberlain 2d A, the St. Louis tornado, and the De Witte hurricane. The ocean cyclone has in addition to these two sources of motion a third, similar to the last, but modified by the fact that the boundary of the stratification between the cold and warm masses instead of being horizontal is vertical in part, as shown by the temperature distributions in cyclones and anticyclones up to 10,000 meters. The land cyclones depend more decidedly upon the third source of motion than does the ocean cyclone.

II.—THE THEORY OF VORTEX MOTION APPLICABLE TO THE DUMB-BELL-SHAPED TUBE IN THE COTTAGE CITY WATERSPOUT.

THE DUMB-BELL-SHAPED TYPE, COTTAGE CITY WATERSPOUT, CHAMBERLAIN 2D A.

An examination of the photographs of the Cottage City waterspout given in the MONTHLY WEATHER REVIEW for July, 1906, pp. 307-315 and Plates I-X, shows that two distinct forms of the tube or types of the vortex were developed at different times from the same cloud. At the second appearance, 1:02 p. m. to 1:17 p. m. (Plates I-VII), the dumb-bell-shaped type prevailed (see Chamberlain's photograph 2d A); and at the third appearance, 1:20 p. m. to 1:27 p. m. (Plates VIII-X), the funnel-shaped type was exhibited. In all accessible photographs of tornadoes these two types occur quite indifferently in numbers, apparently developed by subtle differences in the physical conditions of the cloud at the several occasions of their formation. While both types are of theoretical interest, it is much more important for the meteorologist to understand the dumb-bell type, because the large tornadoes, the hurricanes, and the cyclones in part, are constructed upon the same principles, differing from one another only in their dimensions and proportions. Since the ultimate explanation of the motions of the atmosphere in cyclones and anticyclones seems to be very closely associated with the theory of dumb-bell vortices, it will be proper to keep in mind the goal toward which this present exposition tends.

It can easily be seen in the photographs above referred to, 2d A to 2d G, inclusive (Plates I to VII), that the tube, instead of continuing to taper from the cloud to the sea level, reaches a minimum diameter more than halfway down from the cloud to the sea and then begins to expand. The lower portion is not entirely visible, on account of the enveloping cascade of spray, and it will be shown in these papers that, in fact, the lowest section is not fully developed, and that the vortex tube is amputated or truncated by the sea-level surface at from one-twentieth to one-third of its theoretical length, according to circumstances. The corresponding upper section is fully developed at the cloud, tho the tube and the cloud merge into

one another before the asymptotic extension of the vortex is reached. When the tube begins to break up, and the gyratory velocity diminishes, the dumb-bell form appears more clearly, as on 2d F, and it is very distinct on 2d G. In the earlier numbers of the series, 2d A to 2d E, the inner tubes of the complete vortex, which have very great velocities, are formed, but the outer tubes appear as the rotation velocity falls in amount.

According to the formulas of the first paper of this series (compare Table 3 and Cloud Report, 1898, page 513), we begin with the vortex system expressed as follows:

1. Current function. $\psi = \frac{v\omega}{a} = A\omega^2 \sin az.$
2. Radial velocity. $u = -\frac{1}{\omega} \frac{\partial \psi}{\partial z} = -Aa\omega \cos az.$
3. Tangential velocity. $v = \frac{a\psi}{\omega} = Aa\omega \sin az.$
4. Vertical velocity. $w = \frac{1}{\omega} \frac{\partial \psi}{\partial \omega} = 2A \sin az.$

APPLICATION OF THE FORMULAS TO THE COTTAGE CITY WATERSPOUT, CHAMBERLAIN 2D A.

The primary difference between the funnel-shaped and the dumb-bell-shaped vortex tube is that the former extends from its asymptotic relation at one plane of reference, in the base of the cloud, perpendicularly to a great distance from it, tapering continuously to a tube of very small dimensions, while the latter becomes asymptotic to two planes of reference, one in the cloud base and the other at or below the surface of the sea. Not only is the distance between the two reference planes to be measured in meters, but the axis or connecting line is also to be divided into 180 parts or degrees. Thus, in Fig. 3, assume that the upper line is 1200 meters from the lower line, that the axis is of the same length, and that this represents the entire vortex. If this length is taken as 180° or parts then the a appearing in the formulas is

$$a = \frac{180}{1200} = 0.150 [9.17609],$$

which gives the angular change per meter. Since the symmetry of the formulas, as controlled by the sine and cosine terms, shows that the variations lie between +1 and -1, it follows that $\sin az$ and $\cos az$ will carry the function thru all the intermediate values. Fig. 3 is constructed by plotting the lines determined by the coordinates of Table 17, which gives the radii ω of the several tubes at different heights z .

Since there is no way to determine the value of the tangential velocity at any given point, it is necessary to assume a value for v at a point (ω, z) . The correctness of the one adopted can be checked by constructing the vortex from these data, and comparing it with the shape as shown on the photograph. The height z was determined as about 1200 meters by the measurements, and after several trials I have taken

$$az = 170^\circ \text{ or } 10^\circ,$$

$$\omega = 200 \text{ meters,}$$

$$v = 2 \text{ meters per second.}$$

The value $az = 10^\circ$ is for a point near the sea level, and the value $az = 170^\circ$ is for a point just below the cloud base. Hence we have the current function,

$$a\psi = v\omega = 400 [2.60206].$$

For the value of the ratio of the successive radii, at the points separated by 10-millimeter intervals of pressure, as 760, 750 690, we shall assume the same value as that given on page 469, whose logarithm is,

$$\log \rho = 0.20546.$$

These data enable us to proceed with the computations in the regular order, and to develop the entire structure of this

vortex. It is most convenient to compute the values of ϖ , v , A , u , and w on one selected level, as that for $az = 10^\circ$, and then to extend the computation to the same quantities on the other levels by the use of the formulas 38-49, given in the preceding paper of this series.

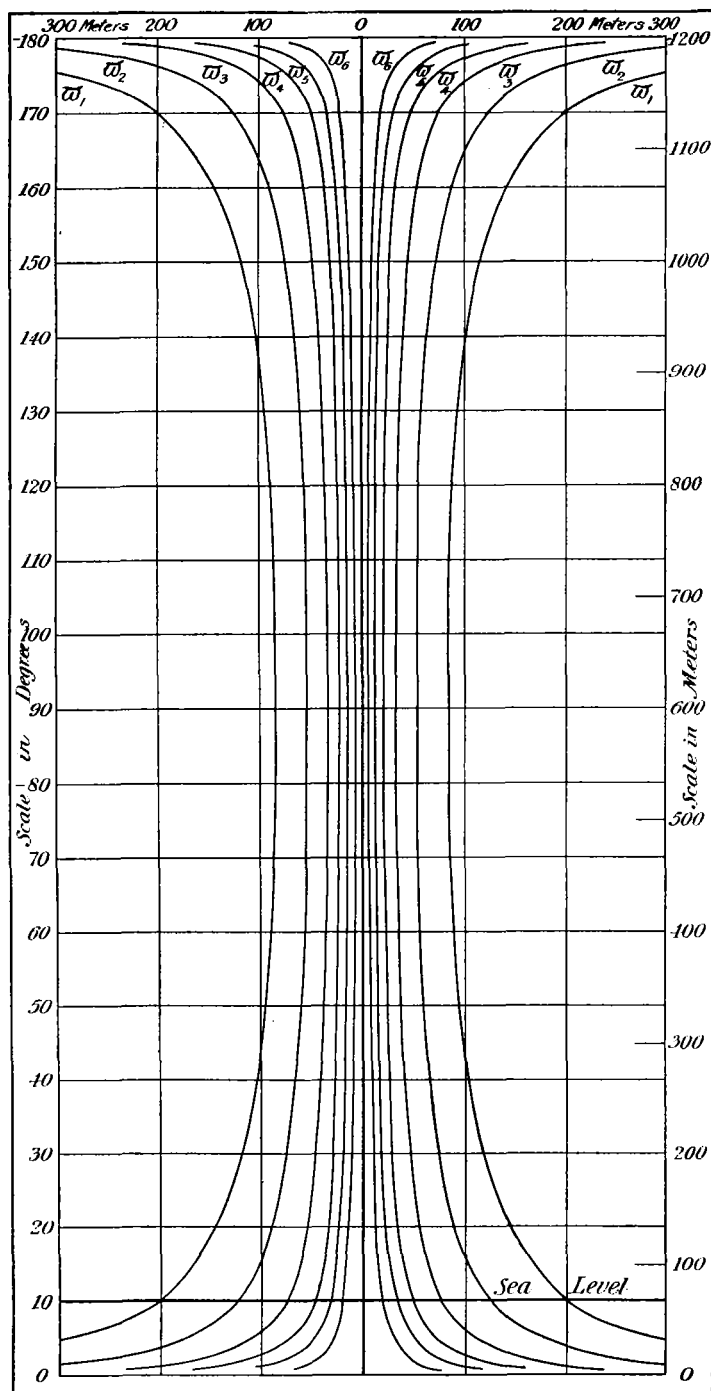


FIG. 3.—Vertical section thru the waterspout, showing the relation between ϖ and z . The tubes ϖ_1 and ϖ_2 are developed only during the time of dissipation of the vortex, and probably tubes ϖ_7 and ϖ_8 are not actually developed in this vortex.

SUMMARY OF THE CONSTANTS FOR THE COMPUTATION ON THE PLANE

$$az = 10^\circ.$$

$$\log a\psi = \log v\varpi = 2.60206$$

$$\log \rho = \log \frac{\varpi_n}{\varpi_{n+1}} = 0.20546$$

$$\log \sin az = \log \sin 10^\circ = 9.23967$$

$$\log \cos az = \log \cos 10^\circ = 9.99335$$

$$\log a \sin az = \log a \sin 10^\circ = 8.41576$$

$$\log a \cos az = \log a \cos 10^\circ = 9.16944$$

$$\log a = \log 0.150 = 9.17609$$

Take the intervals determined by the $\log \rho$ as the points for the computation.

TABLE 13.—The radii of the successive vortex tubes, $\log \varpi_{n+1} = \log \varpi_n - \log \rho = \log \varpi_n - 0.20546$.

	Number of line.*							
	1	2	3	4	5	6	7	8
$\log \varpi$	2.30103	2.09557	1.89011	1.68465	1.47919	1.27373	1.06827	0.86281
ϖ	200.0	124.6	77.6	48.4	30.1	18.8	11.7	7.3

*The word "line" here, and in subsequent tables and text, refers to the numbered lines of figure 3, which represent curved surfaces, bounding successive vortex tubes, taken for purposes of computation.

The successive radii on the same plane are found by subtracting $\log \rho = 0.20546$ from the values in the preceding columns.

TABLE 14.—The tangential velocities, $\log v_{n+1} = \log v + \log \rho = \log v + 0.20546$.

$\log v$	0.30103	0.50649	0.71195	0.91741	1.12287	1.32833	1.53379	1.73925
v	2.0	3.2	5.2	8.3	13.3	21.3	34.2	54.9

The several velocities on the same plane are found by adding $\log \rho = 0.20546$ in succession.

To compute the constant A for each of the successive vortex tubes we construct the values of $\log a\varpi \sin az$ and subtract these values from the logarithms of the corresponding velocities v . The constant A holds for each single special tube, but changes its value from one tube to another.

TABLE 15.—The constant A at the successive vortex tubes.

$\log a \varpi \sin az$..	0.71679	0.51133	0.30587	0.10041	9.89495	9.68949	9.48403	9.27857
$\log A$	9.58424	9.99516	0.40608	0.81700	1.22792	1.63884	2.04976	2.46068
A	0.3839	0.9889	2.5473	6.5614	16.9010	43.5350	112.1400	288.853

In forming the $\log a\varpi \sin az$, the $\log \rho$ is subtracted in succession, and in forming the $\log A$, $2 \log \rho$ is added successively.

To compute the radial velocity u , and the vertical velocity w , the values of $\log Aa\varpi$ and $2A$ are constructed, and $\log \cos az$ and $\log \sin az$ added to them respectively.

TABLE 16.—The radial and vertical velocities for each vortex tube.

	1	2	3	4	5	6	7	8
$\log Aa\varpi$..	1.06136	1.26682	1.47228	1.67774	1.88320	2.08866	2.29412	2.49958
$\log u$	-1.05471	-1.26017	-1.46563	-1.67109	-1.87655	-2.08201	-2.28747	-2.49293
u	11.34	18.20	29.22	46.89	75.26	120.79	193.85	311.12
$\log 2A$..	9.88527	0.29619	0.70711	1.11803	1.52895	1.93987	2.35079	2.76171
$\log w$	9.12494	9.53586	9.94678	0.35770	0.76862	1.17954	1.59046	2.00138
w	0.13	0.34	0.88	2.28	5.87	15.12	38.95	100.32

Having computed the value of $\log u$ under the radius ϖ_1 , the others are found by adding $\log \rho$; and the successive values of $\log w$ are obtained by adding $2 \log \rho$ to the several values in succession. Since the axis of z is positive upward, the movement of the air in the waterspout is continuously positive and therefore upward; the motion of the radial velocity u is inward in the lower half of the vortex, but outward in the upper half of it.

Having thus found the values of $\log \varpi$, $\log u$, $\log v$, and $\log w$ on a given plane of the vortex (in this case the plane which passes thru the point on the axis corresponding to $az = 10^\circ$), it is proper next to extend the computation to other

planes by employing the other values of $\sin az$ and $\cos az$ as required. In order to exhibit the amount of work needed to compute these terms for 10-degree intervals in a vertical direction, and for the stated intervals in a horizontal direction, the computations for $\log w$ and w are given in full, those for u , v , and w requiring similar tables.

TABLE 17.—*Computation of $\log w$ and w for each tube at successive altitudes.*

Values of $\log w$.								
Altitude.	1	2	3	4	5	6	7	8
$az=0^\circ$	∞	∞	∞	∞	∞	∞	∞	∞
10	2.30103	2.09557	1.89011	1.68465	1.47919	1.27373	1.06827	0.86281
20	2.15884	1.94838	1.74292	1.53746	1.33200	1.12654	0.92108	0.71562
30	2.07138	1.86592	1.66046	1.45500	1.24954	1.04408	0.83862	0.63316
40	2.01683	1.81137	1.60591	1.40045	1.19499	0.98953	0.78407	0.57861
50	1.97874	1.77328	1.56782	1.36236	1.15690	0.95144	0.74598	0.54052
60	1.95210	1.74664	1.54118	1.33572	1.13026	0.92480	0.71934	0.51388
70	1.93437	1.72891	1.52345	1.31799	1.11253	0.90707	0.70161	0.49615
80	1.92419	1.71873	1.51327	1.30781	1.10235	0.89689	0.69143	0.48597
90	1.92086	1.71540	1.50994	1.30448	1.09902	0.89356	0.68810	0.48264

Values of the radius w for each tube and altitude.

Altitude.	1	2	3	4	5	6	7	8	C
$az=0^\circ$	∞	∞	∞	∞	∞	∞	∞	∞	
10	200.0	124.6	77.6	48.4	30.1	18.8	11.7	7.3	60
20	142.5	88.8	55.3	34.3	21.5	13.4	8.3	5.2	
30	117.9	73.4	45.8	28.5	17.8	11.1	6.9	4.3	36
40	103.9	64.8	40.4	25.1	15.7	9.8	6.1	3.8	
50	95.2	59.3	37.0	23.0	14.4	8.9	5.6	3.5	34
60	89.6	55.8	34.8	21.6	13.5	8.4	5.2	3.3	
70	86.0	53.6	33.4	20.8	12.9	8.1	5.0	3.1	30
80	84.0	52.3	32.6	20.3	12.7	7.9	4.9	3.06	
90	83.3	51.9	32.4	20.2	12.6	7.8	4.9	3.04	28
100	84.0	52.3	32.6	20.3	12.7	7.9	4.9	3.06	
110	86.0	53.6	33.4	20.8	12.9	8.1	5.0	3.1	30
120	89.6	55.8	34.8	21.6	13.5	8.4	5.2	3.3	
130	95.2	59.3	37.0	23.0	14.4	8.9	5.6	3.5	34
140	103.9	64.8	40.4	25.1	15.7	9.8	6.1	3.8	
150	117.9	73.4	45.8	28.5	17.8	11.1	6.9	4.3	36
160	142.5	88.8	55.3	34.3	21.5	13.4	8.3	5.2	
170	200.0	124.6	77.6	48.4	30.1	18.8	11.7	7.3	68
180	∞	∞	∞	∞	∞	∞	∞	∞	

The last column, marked *C*, in the second portion of Table 17, contains the radius as scaled from the photograph, and it indicates that the vapor tube is a vortex lying a little inside the radius w , on the scale adopted. The radii fluctuate considerably in a natural vortex, as may be seen by comparing Chamberlain 2d A with Coolidge 2d B, 2d F, 2d G, and the selection of the data belonging to a given vortex is not easy, when no observations are available. The barometric pressure in vortices of this type will be considered fully in connection with hurricanes.

THE VELOCITIES IN THE COTTAGE CITY WATERSPOUT.

TABLE 18.—*The radial velocities u for each tube and altitude.*

Altitude.	logs	1	2	3	4	5	6	7	8
$az=0^\circ$	-1.06136	-11.52	-18.49	-29.67	-47.61	-76.42	-122.65	-196.83	-315.92
10	-1.05471	-11.34	-18.20	-29.22	-46.89	-75.26	-120.78	-193.85	-311.12
30	-0.99889	-9.97	-16.01	-25.69	-41.24	-66.18	-106.22	-170.47	-273.59
50	-0.86943	-7.40	-11.88	-19.07	-30.61	-49.12	-78.84	-126.53	-203.07
70	-0.59541	-3.94	-6.32	-10.15	-16.28	-26.14	-41.95	-67.32	-108.05
90	∞	0	0	0	0	0	0	0	0
110	0.59541	3.94	6.32	10.15	16.28	26.14	41.95	67.32	108.05
130	0.86943	7.40	11.88	19.07	30.61	49.12	78.84	126.53	203.07
150	0.99889	9.97	16.01	25.69	41.24	66.18	106.22	170.47	273.59
170	1.05471	11.34	18.20	29.22	46.89	75.26	120.78	193.85	311.12
180	1.06136	11.52	18.49	29.67	47.61	76.42	122.65	196.83	315.92

TABLE 19.—*The tangential velocities v for each tube and altitude.*

$az=0^\circ$	∞	0	0	0	0	0	0	0	0
10	0.30103	2.00	3.21	5.15	8.27	13.27	21.30	34.18	54.86
30	0.76033	5.76	9.24	14.83	23.81	38.21	61.32	98.42	157.97
50	0.94561	8.72	14.16	22.73	36.47	58.54	93.95	150.79	242.01
70	1.03435	10.82	17.37	27.88	44.74	71.81	115.25	184.98	296.87
90	1.06136	11.52	18.48	29.67	47.61	76.42	122.65	196.84	315.92
110	1.03435	10.82	17.37	27.88	44.74	71.81	115.25	184.98	296.87
130	0.94561	8.72	14.16	22.73	36.47	58.54	93.95	150.79	242.01
150	0.76033	5.76	9.24	14.83	23.81	38.21	61.32	98.42	157.97
170	0.30103	2.00	3.21	5.15	8.27	13.27	21.30	34.18	54.86
180	∞	0	0	0	0	0	0	0	0

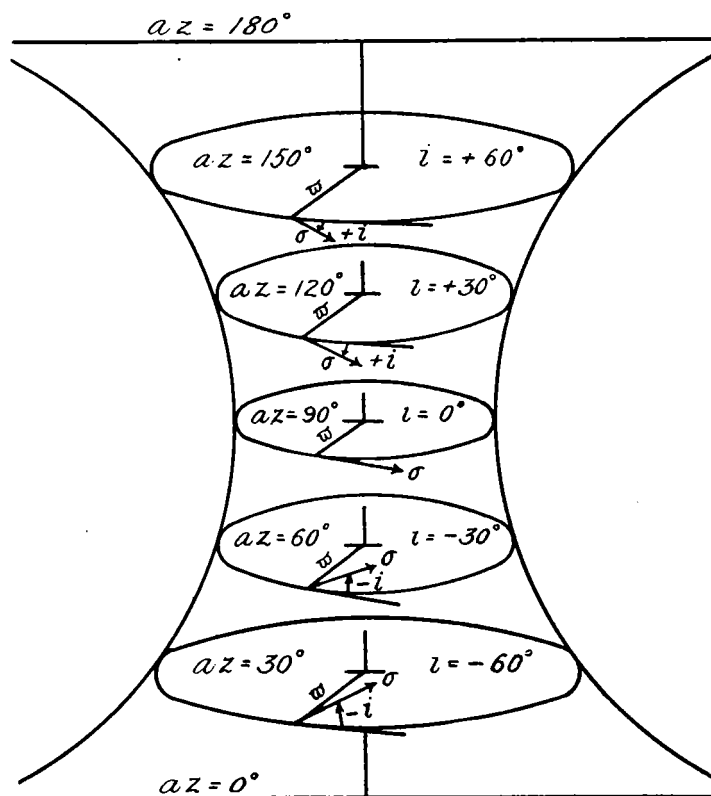
TABLE 20.—*The vertical velocities w for each tube and altitude.*

$az=0^\circ$	∞	0	0	0	0	0	0	0	0
10	9.12494	0.13	0.34	0.88	2.28	5.87	15.12	38.94	100.32
30	9.58424	0.38	0.99	2.54	6.56	16.90	43.54	112.14	288.86
50	9.76952	0.58	1.52	3.90	10.05	25.89	66.70	171.81	442.55
70	9.85826	0.72	1.86	4.79	12.33	31.76	81.82	210.76	542.88
90	9.88527	0.77	1.98	5.10	13.12	33.80	87.07	224.28	577.71
110	9.85826	0.72	1.86	4.79	12.33	31.76	81.82	210.76	542.88
130	9.76952	0.58	1.52	3.90	10.05	25.89	66.70	171.81	442.55
150	9.58424	0.38	0.99	2.54	6.56	16.90	43.54	112.14	288.86
170	9.12494	0.13	0.34	0.88	2.28	5.87	15.12	38.94	100.32
180	∞	0	0	0	0	0	0	0	0

The radial velocity reverses direction at $az=90^\circ$; it is very large in the inner tubes, increasing toward the axis. The tangential velocity is right-handed for upward velocities, so that v and w are both positive for an axis drawn as in fig. 3. The enormous velocities which are developed near the axis, especially the vertical velocity, show where the destructive forces reside that are associated with tornadoes and waterspouts. The hurricane also will develop velocities of a very high order. It is quite probable that the tubes under (1), (2), (7), and (8) did not develop in the vortex of the Cottage City waterspout, tho covered by the computation, which extends beyond the probable limits.

THE HORIZONTAL ANGLE i AND THE VERTICAL ANGLE η OF THE CURRENT q IN THE VORTEX.

As the angles of reference of the current, whose total velocity is q (u , v , w) at the point (w , φ , z), we have taken i and η ; i is the angle between the tangent to the circle whose radius is w and the horizontal component σ , positive outward; η is the angle between σ and q , σ being the projection of q on the horizontal plane. (See fig. 4.)

FIG. 4.—Relations of the angles az and i in the dumb-bell vortex.

$$az=90^\circ+i$$

$$\tan i = \frac{u}{v}, \text{ constant on any plane } az.$$

$$\tan \eta = \frac{w}{v \sec i} \text{ increases from } az=0^\circ \text{ to } az=90^\circ \text{ and from } \sigma_1 \text{ toward the axis.}$$

(Compare fig. 1, page 464.)

The horizontal angle i is directed inward from $az=0^\circ$ to $az=90^\circ$, and outward from $az=90^\circ$ to $az=180^\circ$. This angle i is computed from

$$\tan i = \frac{u}{v},$$

and it is constant on the same plane az .

TABLE 21.—The horizontal angle i , negative inward, positive outward.

Height by angular measure.	1	2	3	4	5	6	7	8
$az=180^\circ$ 0°	0	0	0	0	0	0	0	0
170 10	-90	-90	-90	-90	-90	-90	-90	-90
160 20	-80	-80	-80	-80	-80	-80	-80	-80
150 30	-70	-70	-70	-70	-70	-70	-70	-70
140 40	-60	-60	-60	-60	-60	-60	-60	-60
130 50	-50	-50	-50	-50	-50	-50	-50	-50
120 60	-40	-40	-40	-40	-40	-40	-40	-40
110 70	-30	-30	-30	-30	-30	-30	-30	-30
100 80	-20	-20	-20	-20	-20	-20	-20	-20
90 90	-10	-10	-10	-10	-10	-10	-10	-10
90 90	0	0	0	0	0	0	0	0

The angle i is negative from $az=0^\circ$ to $az=90^\circ$ and positive from $az=90^\circ$ to $az=180^\circ$.

The stream lines are directed toward the axis on the lower asymptotic plane, and gradually incline from the radius as the height, measured by the angle az , increases, so that

$$(50) \quad az=90^\circ + i \text{ or } i=az-90^\circ.$$

When $az=90^\circ$ the angle $i=0^\circ$, and the current is parallel to the circle described by the radius σ , but from that level to $az=180^\circ$, i is positive and becomes 90° for $az=180^\circ$, that is, on the upper asymptotic plane at the base of the cloud. It follows that the angle i can be inferred from the height az above the lower plane, or from measured values of the angle i the height az can be immediately found. If on a given plane, as the sea level, the currents of wind are observed to flow into a vortex at a certain angle, i , measured from the tangent, or at the angle az measured from the radius, it follows that the vortex is truncated by the sea level on that plane, and that the truncating plane can thus be drawn thru a theoretical vortex, this being the plane at which the complete vortex has been cut off by rotating against the surface of the sea.

TABLE 22.—The vertical angle η , $\tan \eta = \frac{w}{v \sec i}$.

Height by angular measure.	1	2	3	4	5	6	7	8
$az=180^\circ$ 0	0 0	0 0	0 0	0 0	0 0	0 0	0 0	0 0
170 10	0 40	1 4	1 42	2 44	4 24	7 2	11 11	17 37
160 20	1 18	2 6	3 22	5 23	8 36	13 39	21 17	32 1
150 30	1 55	3 4	4 55	7 51	12 28	19 33	29 40	42 26
140 40	2 27	3 56	6 18	10 3	15 52	24 32	36 13	49 37
130 50	2 55	4 41	7 30	11 55	18 43	28 32	41 11	54 29
120 60	3 18	5 18	8 28	13 25	20 58	31 35	44 37	57 44
110 70	3 35	5 44	9 10	14 31	22 34	33 43	46 57	59 48
100 80	3 45	6 1	9 36	15 11	23 32	34 57	48 18	60 57
90 90	3 49	6 6	9 45	15 25	23 52	35 22	48 44	61 20

It will be shown that cyclones, hurricanes, and tornadoes develop at the upper plane and extend downward toward the surface, the lower portion of the vortex being destroyed in the working of the tube against the sea or the land surface. Thus in the cyclones the central plane for $az=90^\circ$ is in the strato-cumulus level, where the angle az is about 50° or 60° , making $i=-40^\circ$ or -30° , which is the angle usually measured on the inflowing current. In the hurricane the central plane is somewhat higher, while in the Cottage City waterspout it is about 80° above the sea level, making the inflowing current at the bottom of the cascade construct an angle of 10° from the radius. It is such an action of the dumb-bell vortex in developing the angles in this manner, with the inflowing angle constant on a given plane, and proportional to the height

from the plane of reference, which produces the angles observed in cyclones and hurricanes, rather than the friction k , the deflecting force λ , and the vertical constant c , as was assumed by Ferrel and the German writers in their studies of the problem. We have, therefore, in practise only to measure the velocity and angle of inflow on a given plane, as the land or the sea level, truncate the theoretical vortex at the corresponding plane, and proceed to develop the velocities and angles thruout the entire vortex to the cloud level where it is actually generated.

The angle η is positive from $az=0^\circ$ to $az=180^\circ$. The angle η increases from $az=0^\circ$ to $az=90^\circ$, and it decreases from $az=90^\circ$ to $az=180^\circ$; the angle increases from the outer line toward the axis, and in the middle of the vortex on the plane $az=90^\circ$ at line 8 it may reach about 61° . The $\sec i$ can not be neglected in this computation, as the angle i is of all values from 0° to 90° .

The total velocity can be computed from the formulas,

$$q = (u^2 + v^2 + w^2)^{1/2}, \text{ or } q = v \sec i \sec \eta.$$

TABLE 23.—The total velocity q , in meters per second.

Height by angular measure.	1	2	3	4	5	6	7	8
$az=180^\circ$ 0	11.52	18.49	29.67	47.61	76.42	122.65	196.83	315.47
170 10	11.52	18.49	29.68	47.62	76.64	123.58	200.65	331.47
160 20	11.62	18.50	29.72	47.83	77.29	126.21	211.25	372.60
150 30	11.52	18.51	29.78	48.07	78.26	130.15	226.53	428.05
140 40	11.53	18.53	29.85	48.36	79.45	134.62	243.98	487.61
130 50	11.53	18.55	29.92	48.66	80.69	139.60	261.50	548.81
120 60	11.54	18.56	30.00	48.95	81.84	143.97	276.53	601.77
110 70	11.54	18.58	30.05	49.18	82.75	147.45	288.36	628.04
100 80	11.54	18.59	30.09	49.34	83.35	149.63	295.91	650.63
90 90	11.54	18.59	30.10	49.39	83.56	150.40	298.44	658.57

The visible vortex, as it develops in the atmosphere, is probably confined within the lines 3, 4, 5, and 6, tho possibly extending a little beyond σ_6 .

The volume of air V , in cubic meters per second, which passes upward thru each vortex tube, is computed from the formula,

$$V = \pi (\sigma_n^2 - \sigma_{n+1}^2) w_m = \text{a constant},$$

w_m being the mean velocity, as obtained by the formula,

$$\log w_m = \frac{1}{2} (\log w_n + \log w_{n+1}).$$

The value of V is computed for three levels, and the result is given in Table 24, taking the values of $\log \sigma$ and $\log w$ from Tables 17 and 20.

TABLE 24.—The volume of air ascending in each vortex tube.

Height of stratum.	1-2	2-3	3-4	4-5	5-6	6-7	7-8
$az=10^\circ$	16451.5	16451.5	16451.5	16451.5	16451.5	16451.5	16451.5
$az=30^\circ$	16451.5	16451.5	16451.5	16451.5	16451.5	16451.5	16451.5
$az=90^\circ$	16451.5	16451.5	16451.5	16451.5	16451.5	16451.5	16451.5

In the funnel-shaped vortex it was found that the volume of ascending air was 2467.7 cubic meters per second, so that the dumb-bell vortex is carrying 6.666 times as much air upward as the funnel-shaped vortex. It may be inferred that the change from one type of vortex to the other is due to the requirements of the temperature conditions at the cloud, the greater changes due to the overflowing cold sheet demanding a stronger upflow in the dumb-bell vortex, the smaller changes in temperature in the horizontal sheet being satisfied by the feebler action of the funnel-shaped vortex. This becomes equivalent to the statement that at the immediate base of the cloud the horizontal velocity u is stronger in the dumb-bell vortex than in the funnel-shaped vortex.

EVALUATION OF THE EQUATIONS OF MOTION.

In the future chapters we shall fully consider all the forces and conditions that appreciably affect vortex motions, but for the present we shall consider only the simplified equations of motion that apply to the case of no inertia, no friction, and no deflecting force. In this case the equations of motion of a vortex (see No. (6), page 465, or Cloud Report, 1898, page 504, equation 200, and page 502, equation 180) become,

$$\begin{cases} (1) & -\frac{\partial P}{\rho \partial \sigma} = u \frac{\partial u}{\partial \sigma} + w \frac{\partial u}{\partial z} - \frac{v^2}{\sigma}, \\ (2) & 0 = u \frac{\partial v}{\partial \sigma} + w \frac{\partial v}{\partial z} + \frac{uv}{\sigma}, \\ (3) & -\frac{\partial P}{\rho \partial z} = u \frac{\partial w}{\partial \sigma} + w \frac{\partial w}{\partial z} + g. \end{cases}$$

The partial differentials of the velocity in the direction of the radius σ and the vertical z can be computed in terms of the constants of the vortex, from the equation for the current function,

$$\psi = A \sigma^2 \sin az.$$

Thus we find the partial differentials of the velocities as follows:

$$(51) \quad \begin{cases} u = -A a \sigma \cos az, & v = A a \sigma \sin az, & w = 2 A \sin az. \\ \frac{\partial u}{\partial \sigma} = -A a \cos az, & \frac{\partial v}{\partial \sigma} = A a \sin az, & \frac{\partial w}{\partial \sigma} = 0. \\ \frac{\partial u}{\partial z} = A a^2 \sigma \sin az, & \frac{\partial v}{\partial z} = A a^2 \sigma \cos az, & \frac{\partial w}{\partial z} = 2 A a \cos az. \end{cases}$$

The products of these quantities are then formed as follows:

$$(52) \quad \begin{cases} u \frac{\partial u}{\partial \sigma} = A^2 a^2 \sigma \cos^2 az, & u \frac{\partial u}{\partial z} = 2 A^2 a^2 \sigma \sin^2 az, \\ u \frac{\partial v}{\partial \sigma} = -A^2 a^2 \sigma \sin az \cos az, & u \frac{\partial v}{\partial z} = 2 A^2 a^2 \sigma \sin az \cos az, \\ u \frac{\partial w}{\partial \sigma} = 0, & u \frac{\partial w}{\partial z} = 4 A^2 a \sin az \cos az, \\ \frac{v^2}{\sigma} = A^2 a^2 \sigma \sin^2 az, & \frac{uv}{\sigma} = -A^2 a^2 \sigma \sin az \cos az. \end{cases}$$

Hence, the three equations of motion as above given reduce to,

$$(53) \quad \begin{cases} (1) & -\frac{\partial P}{\rho \partial \sigma} = A^2 a^2 \sigma, \\ (2) & 0 = 0. \\ (3) & -\frac{\partial P}{\rho \partial z} = g + 4 A^2 a \sin az \cos az. \end{cases}$$

The second equation reduces to zero.

AN EXAMPLE.

TABLE 25—Collection of the data for an example in computing the equations of motion for any special radius σ and level az .

Data.	1	2	3	4	5	6	7	8
log $A \dots$	9.58424	9.99516	0.40608	0.81700	1.22792	1.63884	2.04976	2.46068
$A \dots$	0.3839	0.9839	2.5473	6.5614	16.9010	43.5350	112.140	288.853
log $\sigma_{10} \dots$	2.30103	2.09557	1.89011	1.68465	1.47919	1.27373	1.06827	0.86281
$\sigma_{20} \dots$	2.15384	1.94838	1.74292	1.53746	1.33200	1.12654	0.92108	0.71562
$\sigma_{10} \dots$	200.0	124.6	77.6	48.4	30.1	18.8	11.7	7.3
$\sigma_{20} \dots$	142.5	88.8	55.3	34.3	21.5	13.4	8.3	5.2
log $u_{10} \dots$	-1.05471	-1.26017	-1.46563	-1.67109	-1.87655	-2.08201	-2.28747	-2.49293
$u_{20} \dots$	-1.03435	-1.23981	-1.44527	-1.65073	-1.85619	-2.06165	-2.26711	-2.47257
$u_{10} \dots$	-11.34	-18.20	-29.22	-46.89	-75.26	-120.78	-193.85	-311.12
$u_{20} \dots$	-10.82	-17.37	-27.88	-44.74	-71.81	-115.25	-184.93	-296.86
log $v_{10} \dots$	0.30103	0.50649	0.71195	0.91741	1.12287	1.32833	1.53379	1.73925
$v_{20} \dots$	0.59541	0.80087	1.00633	1.21179	1.41725	1.62271	1.82817	2.03363
$v_{10} \dots$	2.00	3.21	5.15	8.27	13.27	21.30	34.18	54.86
$v_{20} \dots$	3.94	6.32	10.15	16.29	26.14	41.95	67.32	108.05
log $w_{10} \dots$	9.12494	9.53586	9.94678	0.35770	0.76862	1.17954	1.59046	2.00138
$w_{20} \dots$	9.41932	9.83024	0.24116	0.65208	1.06300	1.47392	1.88484	2.29576
$w_{10} \dots$	0.13	0.34	0.88	2.28	5.87	15.12	38.94	100.32
$w_{20} \dots$	0.26	0.68	1.74	4.49	11.56	29.78	76.71	197.59

An example of the practical working of these equations may be taken from the data of the preceding tables, which are collected for convenience in Table 25. The point selected is on the level $az=10^\circ$ and between the radii σ_3 and σ_4 , intending to integrate across the tube $\sigma_3-\sigma_4$ at the level $az=10^\circ$ and vertically thru this point from $az=5^\circ$ to $az=15^\circ$.

The interpolations are to be made at the middle point of the tube ($\sigma_3-\sigma_4$) and on the plane $az=10^\circ$.

The arrangement of the computations for each side of each equation (thus checking the theory from two points of view) is as follows:

$$u \frac{\partial u}{\partial \sigma} = A^2 a^2 \sigma \cos^2 az.$$

Left-hand term.			Right-hand term.	
Term.	Number.	Logarithm.	Term.	Logarithm.
u_m	-37.01	-1.56836	A^2	1.22308
$\frac{\partial u}{\partial \sigma}$	-17.67	-1.24724	a^2	8.35218
σ	+29.20	1.46528	σ	1.78738
			$\cos^2 az$	9.98670
$u \frac{\partial u}{\partial \sigma}$	22.40	1.35022		
			22.35	1.34934

$$u \frac{\partial v}{\partial \sigma} = -A^2 a^2 \sigma \sin az \cos az.$$

Left-hand terms.			Right-hand terms.	
Term.	Number.	Logarithm.	Term.	Logarithm.
u_m	-37.01	-1.56836	$-A^2 a^2 \sigma$	-1.36264
$\frac{\partial v}{\partial \sigma}$	+3.12	0.49415	$\sin az$	9.23967
$\frac{\partial v}{\partial \sigma}$	+29.20	1.46538	$\cos az$	9.99335
$u \frac{\partial v}{\partial \sigma}$	-3.955	-0.59713		
			-3.942	-0.59556

$$u \frac{\partial w}{\partial \sigma} = 0.$$

u_m	-37.01	-1.56836	}	0
$\frac{\partial w}{\partial \sigma}$	+1.40	0.14613		
$\frac{\partial w}{\partial \sigma}$	+29.20	1.46538		
$u \frac{\partial w}{\partial \sigma}$	-1.775	-0.24911	0	

This discrepancy results from the fact that $\frac{\partial w}{\partial \sigma}$ has a value $\frac{1.40}{29.20} = 0.05$, slightly larger than 0.

In evaluating the partial differentials in the direction of the angular coordinate az , the factor $57^\circ.29578$ must be introduced into the terms for partial differential, as this is the number of degrees in one radius. Since the angular distance is 180 degrees and the linear distance 1200 meters, the 10-degree interval is equivalent to

$$\partial z = 10\text{-degree interval} = \frac{1200}{18} \cdot \frac{1}{57.29578} = 1.1636,$$

which is the value of ∂z in the partial differentials.

$$w \frac{\partial u}{\partial z} = 2 A^2 a^2 \sigma \sin^2 az.$$

Left-hand terms.			Right-hand terms.	
Term.	Number.	Logarithm.	Term.	Logarithm.
w_m	+1.42	0.15224	2	0.30103
$\frac{\partial u}{\partial z}$	1.14	0.05690	$A^2 a^2 \sigma$	1.36264
$\frac{\partial u}{\partial z}$	1.1636	0.06579	$\sin^2 az$	8.47934
$w \frac{\partial u}{\partial z}$	1.391	0.14335	1.390	0.14301

$$w \frac{\partial v}{\partial z} = 2 A^2 a^2 \sigma \sin az \cos az.$$

w_m	1.42	0.15224	$2 A^2 a^2 \sigma$	1.66367
$\frac{\partial v}{\partial z}$	6.452	0.80969	$\sin az$	9.23967
$\frac{\partial v}{\partial z}$	1.1636	0.06579	$\cos az$	9.99335
$w \frac{\partial v}{\partial z}$	7.873	0.89614	7.883	0.89669

$$w \frac{\partial w}{\partial z} = 4 A^2 a \sin az \cos az.$$

w_m	1.42	0.15224	$4 A^2 a$	1.00123
$\frac{\partial w}{\partial z}$	1.404	0.14737	$\sin az$	9.23967
$\frac{\partial w}{\partial z}$	1.1636	0.06579	$\cos az$	9.99335
$w \frac{\partial w}{\partial z}$	1.713	0.23382	1.715	0.23425

$$\frac{v^2}{\sigma} = A^2 a^2 \sigma \sin^2 az.$$

$\frac{v^2}{\sigma}$	42.59	1.62936	$A^2 a^2 \sigma$	1.36264
	61.29	1.78738	$\sin^2 az$	8.47934
$\frac{v^2}{\sigma}$	0.695	9.84198	0.695	9.84198

$$\frac{uv}{\sigma} = -A^2 a^2 \sigma \sin az \cos az.$$

u	-37.01	-1.56836	$-A^2 a^2 \sigma$	-1.36264
v	6.526	0.81468	$\sin az$	9.23967
σ	61.29	1.78738	$\cos az$	9.99335
$\frac{uv}{\sigma}$	-3.941	-0.59566	-3.941	-0.59566

With these values, our equations of motion for the vortex tube, (3)-(4), now become

- (1) $-\frac{\partial P}{\rho \partial \sigma} = 22.35 + 1.390 - 0.695 = 23.04 = A^2 a^2 \sigma.$
- (2) $0 = -3.942 + 7.883 - 3.941 = 0.$
- (3) $-\frac{\partial P}{\rho \partial z} = -1.775 + 1.715 + g = 9.746,$

since $g = 9.806$ at 45° latitude and sea level.

In making the several interpolations for u_m , v_m , w_m , A_m , in preparation for the integration across the intervals $\partial \sigma$ and ∂z the mean values as derived from the mean logarithms were employed. There are several small differences between the above results obtained by computing both sides of the equations independently, but these are largely due to the neglect of the second differentials, because the curves between the initial and final points were not followed exactly in this integration. The terms in the A_m are more accurate than the others, as here computed.

The pressure at the sea-level plane.

The computation of the pressure at the level defined by $az = 10^\circ$, that is the assumed sea level, is made by the formula,

$$P_n - P_{n+1} = \rho_m A^2 a^2 \sigma (\sigma_n - \sigma_{n+1}),$$

which is easily deduced from the first equation of motion (equation 53),

$$-\frac{\partial P}{\rho \partial \sigma} = A^2 a^2 \sigma,$$

and gives the results found in Table 26.

TABLE 26.—Fall in pressure between the successive vortex rings.

Rings.	1-2	2-3	3-4	4-5	5-6	6-7	7-8
$A^2 a^2 \sigma$	1.349	5.575	23.05	95.28	393.91	1628.5	6732.3
$\sigma_n - \sigma_{n+1}$	75.4	47.0	29.2	18.3	11.3	7.1	4.4
ρ_m	1.2682	1.2682	1.2682	1.2682	1.2682	1.2682	1.2682
$P_n - P_{n+1}$	126.0	332.3	853.5	2211.3	5645.0	14663.	37563.
$B_n - B_{n+1}$	0.94	3.49	6.40	16.58	42.34	110.0	281.7

When a waterspout descends to sea level it is equivalent to assuming that the pressure falls at the core by the amount of the computed difference in pressure between the sea level and the base of the cumulus cloud, or, in this case, 91 millimeters. Starting from the assumed outer ring (3), we compute the difference of the barometric pressure, $6.40 + 16.58 + 42.34 + 26.00 = 91.32$ millimeters. Hence, it follows that the calm core is to be limited at about 16 meters, as can be seen by comparing Table 26 with the radii σ of the rings in Table 25, since the 26.00 millimeters of pressure must be distributed beyond σ_6 in the direction of σ_r .

THE CASCADE OF THE COTTAGE CITY WATERSPOUT.

The photographs, Chamberlain 2d A in particular, show that the bottom of the tube near the ocean is surrounded by a vaporous mass of rounded form, which I have analyzed as follows: The vortex tube approaches the sea level with violent radial, tangential and vertical components of velocity, sharply separated from the quiet air surrounding it, at the outermost layer of the revolving vortex. Were there no ocean or obstacle to disturb the vortex motion, and were the tube to form in a frictionless medium, the tube would extend to the asymptote at a given distance, leaving a small calm core free from gyration. But in fact the tube encounters the waters of the ocean, and becomes distorted by the action of the conflicting forces. The most prominent effect is the change in the size of the tube, and the decrease of gyratory velocity in consequence of friction and the other forces, caused by the transfer of the energy of the tube to the masses of air and water, wherein the forces of inertia are very large, since quiet air and water are suddenly set in violent motion on meeting the vortex. The intake of the vortex, due to the strong ascending helical motion, requires a supply of air which enters the tube by curved paths, as shown on the photograph by the clear spaces near the surface of the ocean. The water itself leaps up a few feet at the center into a point, or conical wave, and a sharp measure of this distance is desirable as the pressure-fall in the center of the tube can be estimated from it. The circular rotation of the tube at the surface cuts up the water into drops of spray, which are drawn into the tube, together with the air moving toward the axis.

At a certain height above the surface where the intake has become satisfied, and there are only small radial components setting inward, the water and spray are thrown by the centrifugal and deflecting forces outward from the tube at the height of about 110 meters. This mass of air and water inside the tube is gyrating violently, but on being ejected from the tube it impinges upon the quiet air and loses its projectile energy upward and outward, so that it falls back to the ocean in a cascade. The falling spray is again sucked into the tube on approaching the levels where the intake begins, and the orbital rotation may be thus repeated more than once. It is evident that there is a series of beautiful mechanical problems in this connection, but it is not easy to treat them fully, because the size of the drops, the action of viscosity on the velocity, and the velocity components themselves are not fully known. Since the formulas for the vortex apply to media without friction and to parabolic trajectories, it is difficult to modify them to meet the actual atmospheric conditions. There is evidently a right-hand and a left-hand trajectory, so that the origin of coordinates (x, z) can be taken at the axis of the vortex as it touches the water; x is along the surface, and z is perpendicular to it along the axis of the tube. I have written down the formulas for the parabolic trajectories, which can be readily understood from fig. 5.

Some computations of a parabola thru the points ($x=0, z_1=0$) and ($x_2=55, z_2=128$) show that this parabola is too sharp near the vortex for the trajectory of the spray, and accordingly some other curves have been sketched in, showing the boundary of the water cascade, and some arrows indicating

the paths of the water drops, the spray and the air, which seem to conform to the design on Chamberlain's photograph. To pass from the pure parabola to the actual paths of the water and spray masses is probably quite impracticable by mathematical analysis, till we know more of the size of the water masses, the viscosity, and the actual velocities in the several parts of the disturbed tube, especially in the stream lines near the surface where the vortex forces are seriously disturbed by composition with the inflowing masses, suddenly changed from rest into violent motion. It is evident that all waterspouts and tornadoes will suck in objects near the surface, and discharge them into the quiet air a few hundred feet above the surface, when they will fall again.

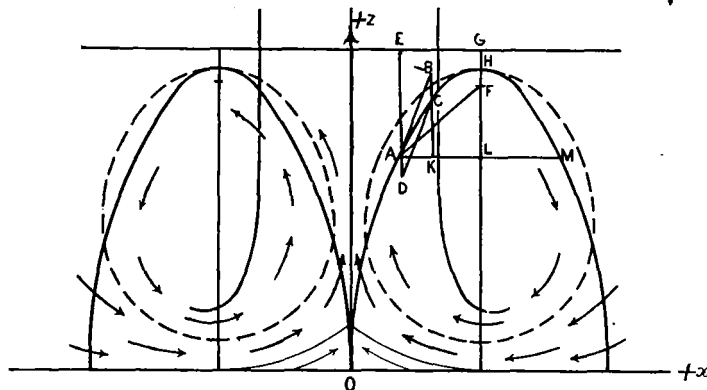


FIG. 5.—Circulation of air and water in cascade. Heaviest full lines, vortex tube. Middle full lines, parabolic trajectories. Lightest full lines, water cone. Dotted ovals, paths of water drops in cascade. Arrows, direction of circulation. Height of cascade = 128 meters. Diameter of cascade = 220 meters. Diameter of vortex tube = 74 meters.

TABLE 27.—Formulas for parabola.

$$\begin{aligned} AB &= vt, \\ \overline{AB^2} &= v^2 t^2, & AB^2 &= \frac{2v^2}{g} \cdot AD, \\ BC &= \frac{1}{2} gt^2, \\ AF &= AE = h, & v^2 &= 2gh, \\ FH &= GH, \\ EAB &= BAF, & \overline{AB^2} &= 4h \cdot AD, \\ BAL &= a. \end{aligned}$$

TABLE 28.—Equations of parabola.

$$\left. \begin{aligned} AK &= x = vt \cos a, \\ BK &= vt \sin a, \\ BC &= \frac{1}{2} gt^2, \\ CK &= z = vt \sin a - \frac{1}{2} gt^2. \end{aligned} \right\} \text{origin at } A.$$

$$\begin{aligned} z &= x \tan a - \frac{gx^2}{2v^2 \cos^2 a}, \\ z &= x \tan a - \frac{x^2}{4h \cos^2 a} \end{aligned}$$

TABLE 29.—Formulas for the angle a , height h , and velocity v (in vacuo) of a parabola thru (x_1, z_1), (x_2, z_2).

$$\left. \begin{aligned} z_1 &= x_1 \tan a - \frac{x_1^2}{4h \cos^2 a}, \\ z_2 &= x_2 \tan a - \frac{x_2^2}{4h \cos^2 a}, \end{aligned} \right\} \text{origin at } O.$$

$$\tan a = \frac{z_1 x_2 - z_2 x_1}{x_1 x_2 (x_2 - x_1)},$$

$$h = \frac{x_1 x_2 (x_2 - x_1)}{4 \cos^2 a (z_1 x_2 - z_2 x_1)},$$

$$v^2 = 2gh = \frac{1}{4 \cos^2 a} \cdot \frac{2gx_1 x_2 (x_2 - x_1)}{z_1 x_2 - z_2 x_1},$$

$$\text{Range } AM = 4h \cos a \sin a = 2h \sin 2a,$$

$$\text{Time of flight} = t = \frac{4h \sin a}{v} = \frac{2v \sin a}{g},$$

$$\text{Greatest height} = HL = h \sin^2 a. \quad \left. \vphantom{\frac{2v \sin a}{g}} \right\} \text{origin at } A.$$